Legends for Supplemental Figures

Supplemental Figure 1. NMDAR sparklets are inhibited by the NMDAR pore blocker MK-801.

L

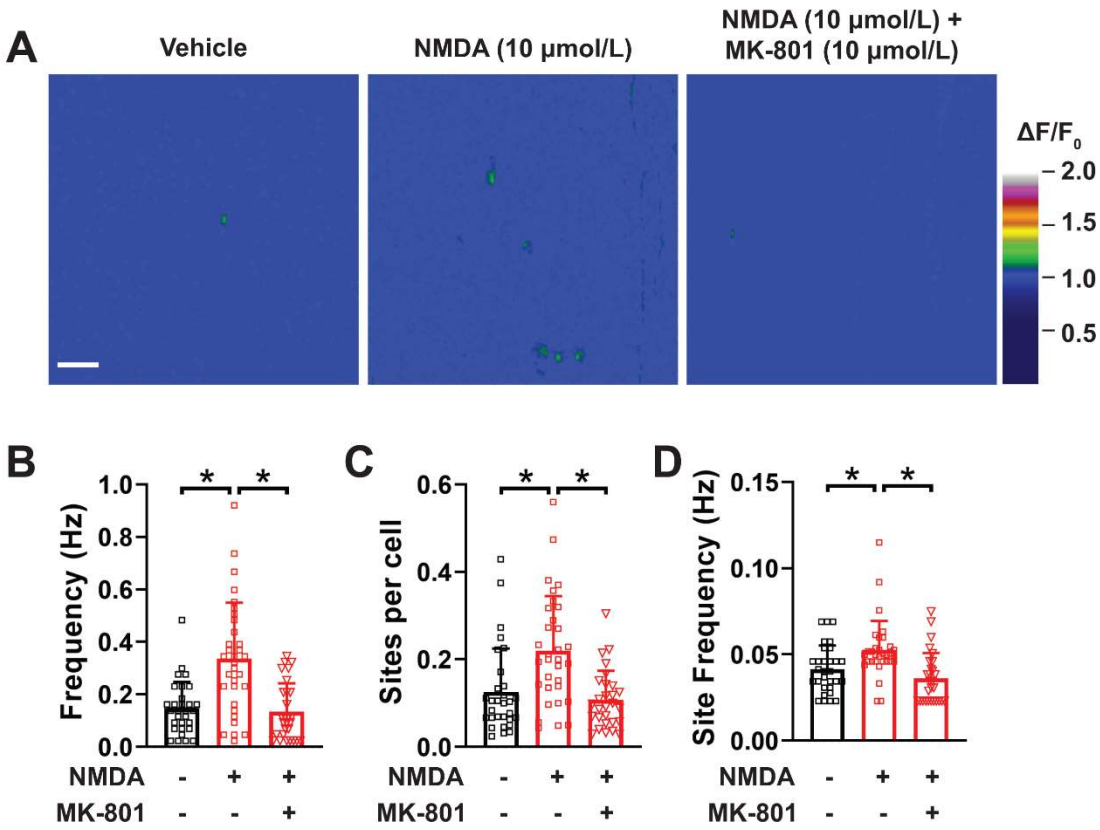

Supplemental Figure 1. *NMDAR sparklets are inhibited by the pore-blocking antagonist MK-801.* **(A)** Pseudocolored images of fields of view from *en face* cerebral arteries preparations from *cdh5:Gcamp8* mice showing the increase in number of active sites of NMDAR sparklets after exposure to NMDA (middle panel), an effect blocked by MK-801 (right panel). Bar = 20 µm. **(B-D)** Summary graphs showing that MK-801 prevents the increase in *NMDAR sparklets* frequency **(B)**, active sites per cell **(C)** and site frequency **(D)** in cerebral artery endothelial cells. *p<0.05, Brown-Forsithe test with a Dunnet's T3 correction for multiple comparisons. A total of 4 preparations were analyzed, isolated from 2 male and 2 female mice.

Supplemental Figure 2. Removal of extracellular Ca^{2+} abolished *NMDAR sparklets*.

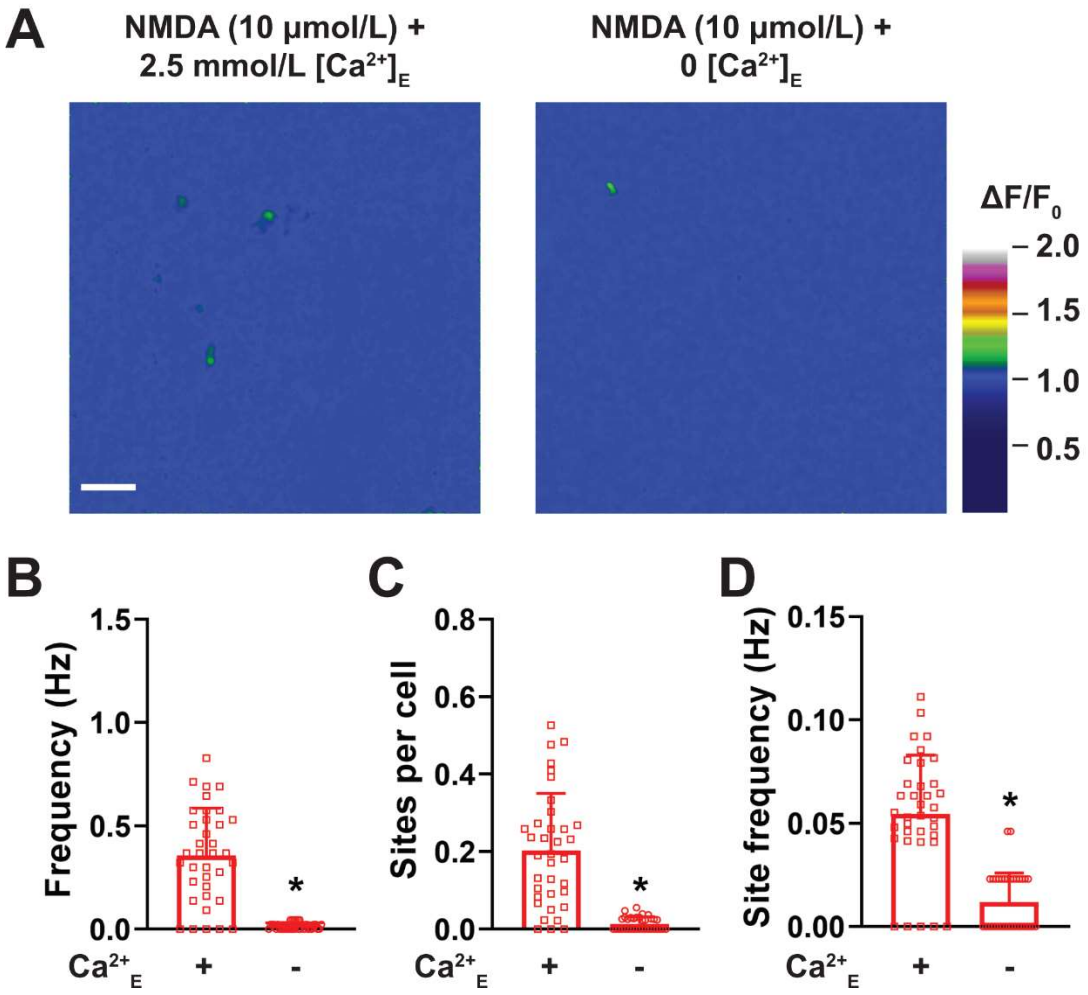

Supplemental Figure 2. *Removal of extracellular Ca^{2+} abolishes NMDAR sparklets.* **(A)** Representative pseudocolored $\Delta F/F_0$ rendering of fields of views of cerebral arteries exposed to imaging PSS containing extracellular Ca^{2+} (Ca^{2+}_E, 2.5 mmol/L, left) or without extracellular Ca^{2+} (right). Bar = 20 µm. **(B-D)** Summary bar graphs showing that removal of extracellular Ca^{2+} almost completely abolished *NMDAR sparklets* frequency in the entire field of view **(B)**, number of sites per cell **(C)** and frequency of events in single sites **(D)**. Data are means ± SD, n = 36-36 fields of view from 3 different preparations isolated from 3 *cdh5:Gcamp8* mice (1 male and 2 female). *p < 0.05, two-tailed Mann-Whitney test.

Supplemental Figure 3. Properties of *NMDAR sparklets*

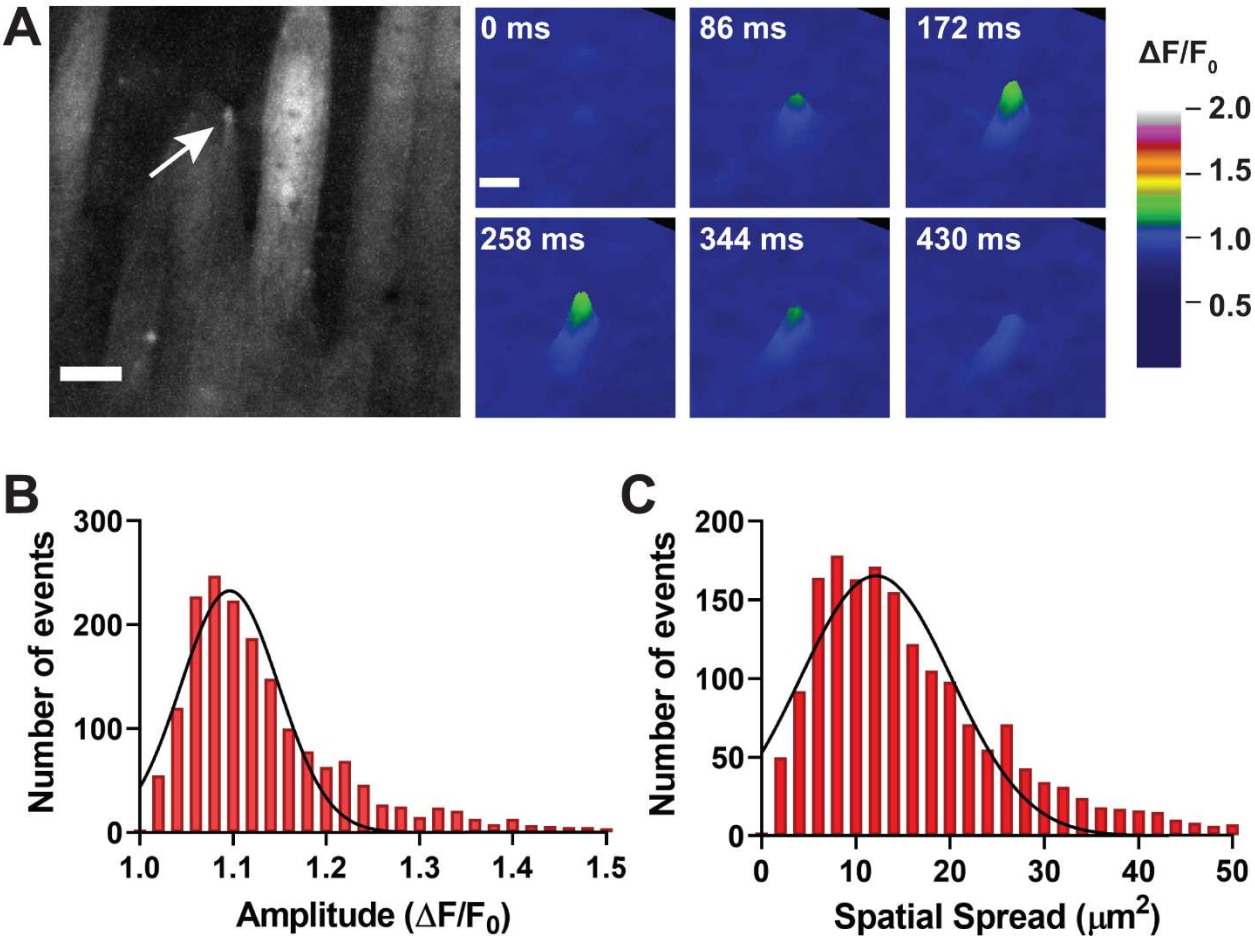

Supplemental Figure 3. *Biophysical characteristics of NMDAR sparklets.* **(A)** Representative pseudcolored timelapse of the 3-dimensional rendering of a *NMDAR sparklet*. The greyscale image showing the 2-dimensional recording of the *NMDAR sparklet* is on the left. Bar = 10 μm for grayscale image and 3 μm for pseudocolored image. **(B)** Frequency distribution plot of amplitudes of *NMDAR sparklets* showing a Gaussian distribution with mode at 1.08 $\Delta F/F_0$. A total of 1783 events were analyzed. **(C)** Frequency distribution plot of 2-dimensional spatial spreads of *NMDAR sparklets* with a single modal Gaussian distribution at 7.5 μm^2. A total of 1783 events were analyzed.

Supplemental Figure 4. Modalities and properties of intracellular Ca^{2+} transients in endothelial cells induced by NMDA.

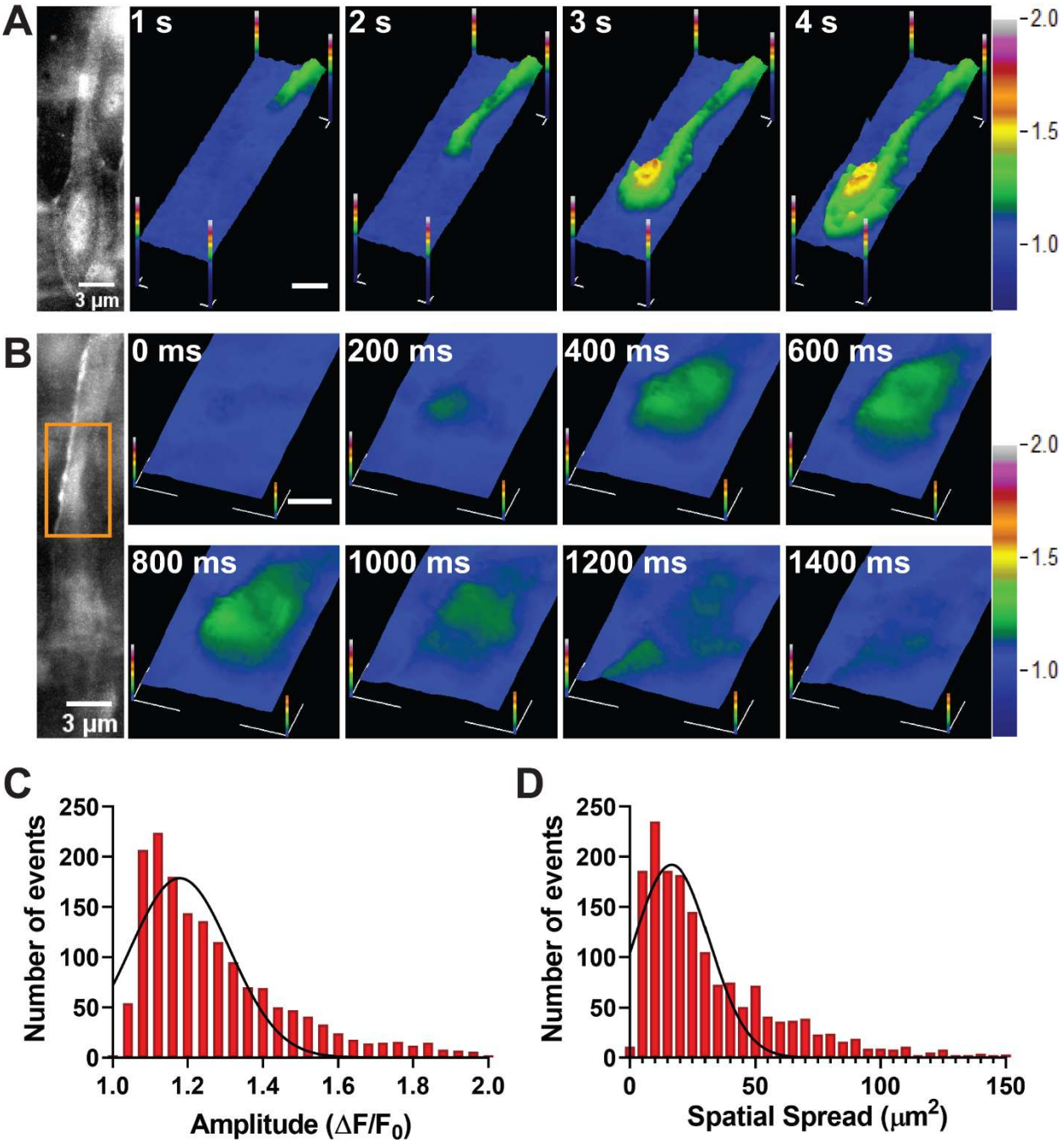

Supplemental Figure 4. *Modalities and properties of intracellular Ca^{2+} transients induced by NMDA.* **(A)** Depiction of cellular increase in Ca^{2+}, observed as a propagating Ca^{2+} wave. Note that the event starts in one end of the cell and propagates through the entire

cell length. The image on the leftmost panel is the grayscale format of the pseudocolored panels. **(B)** Depiction of a larger and more robust, albeit subcellular, increase in intracellular Ca^{2+}. The majority of such events is likely composed of release of Ca^{2+} from intracellular stores. **(C)** Frequency distribution plot of amplitudes of NMDA-induced Ca^{2+} transients showing a Gaussian distribution with mode at 1.12 $\Delta F/F_0$. A total of 1637 events were analyzed. **(D)** Frequency distribution plot of 2-dimensional spatial spreads of NMDA-induced Ca^{2+} transients with a single modal Gaussian distribution at 10 μm^2. A total of 1637 events were analyzed.

Supplemental Figure 5. MK-801 reduces the frequency of intracellular Ca^{2+} transients and number of active sites per cell.

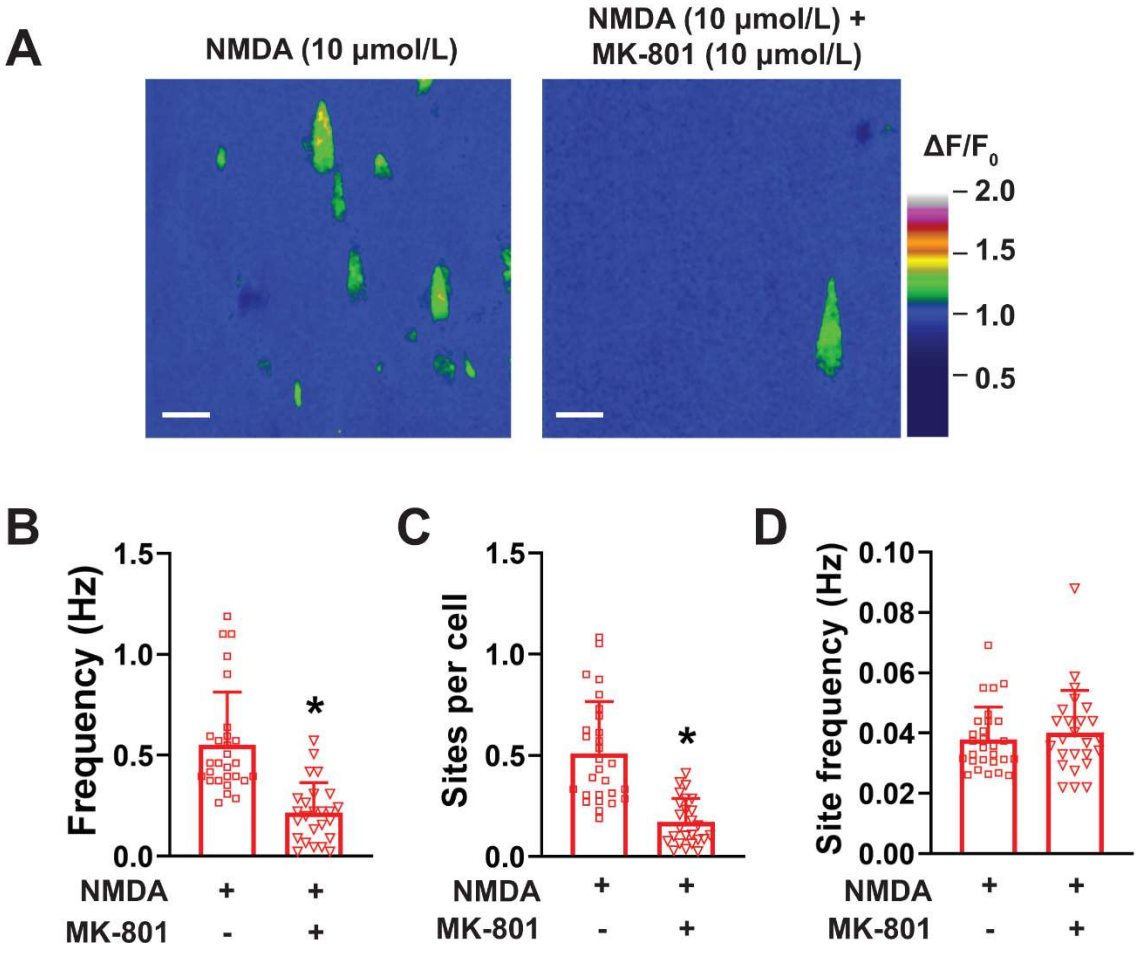

Supplemental Figure 5. *MK-801 reduces frequency of calcium transients and number of active sites per cell.* **(A)** Pseudocolored images of fields of view from *en face* cerebral arteries preparations from *cdh5:Gcamp8* mice showing the number of active sites of NMDAR-induced calcium transients after exposure to NMDA (left panel), an effect blocked by MK-801 (right panel). Bar = 20 μm. **(B-D)** Summary graphs showing that MK-801 reduces NMDAR-induced intracellular Ca^{2+} transient, observed as a decrease in frequency **(B)** and active sites per cell **(C)**, with no significant change to site frequency **(D)**, in cerebral artery endothelial cells. Data are means ± SD, n = 28-25 fields of view from 3 different preparations isolated from 3 *cdh5:Gcamp8* mice (1 male and 2 female). *p < 0.05, two-tailed Mann-Whitney test.

Supplemental Figure 6. Absence of sex differences in EC Ca^{2+} responses to NMDA.

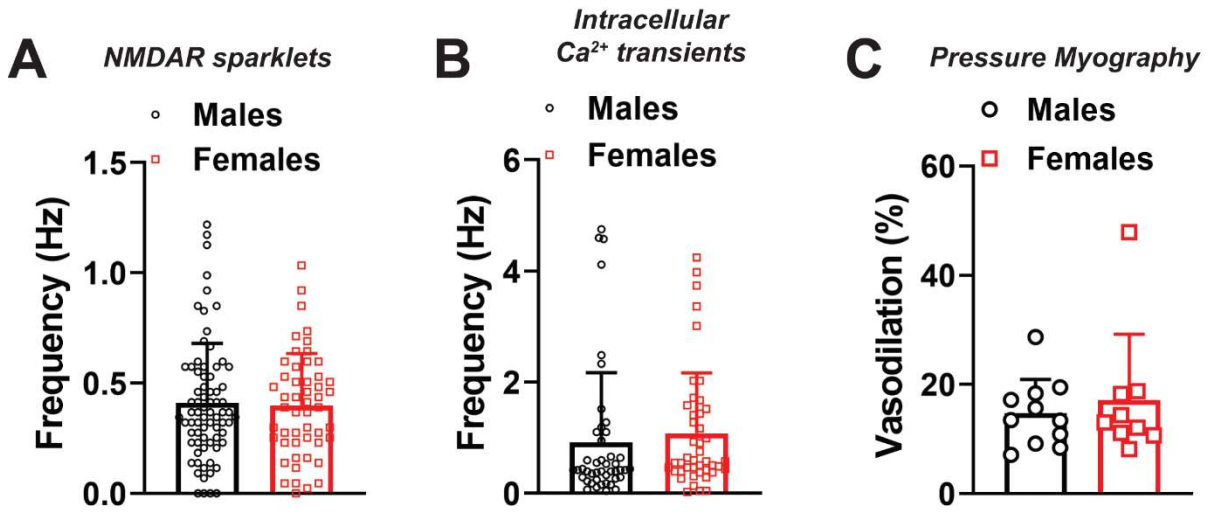

Supplemental Figure 6. *Absence of sex differences in EC calcium responses to NMDA.* **(A)** Summary bar graph showing that no significant differences were observed between biological sexes for frequency of *NMDAR sparklets*. Data are means ± SD, n = 74-51 fields of view from 14 different preparations isolated from 11 *cdh5:Gcamp8* mice (6 male

and 5 female). **(B)** Similarly, no significant differences were observed between males and females in the frequency of NMDAR-induced Ca^{2+} transients. Data are means ± SD, n =45-44 fields of view from 9 different preparations isolated from 9 *cdh5:Gcamp8* mice (5 male and 4 female). **(C)** PComA dilation to NMDA was not different between males and females. Data are means ± SD, n = 11-9 preparations isolated from 11 *cdh5:Gcamp8* mice (7 male and 4 female).

Supplemental Figure 7. Number of cells per field of view.

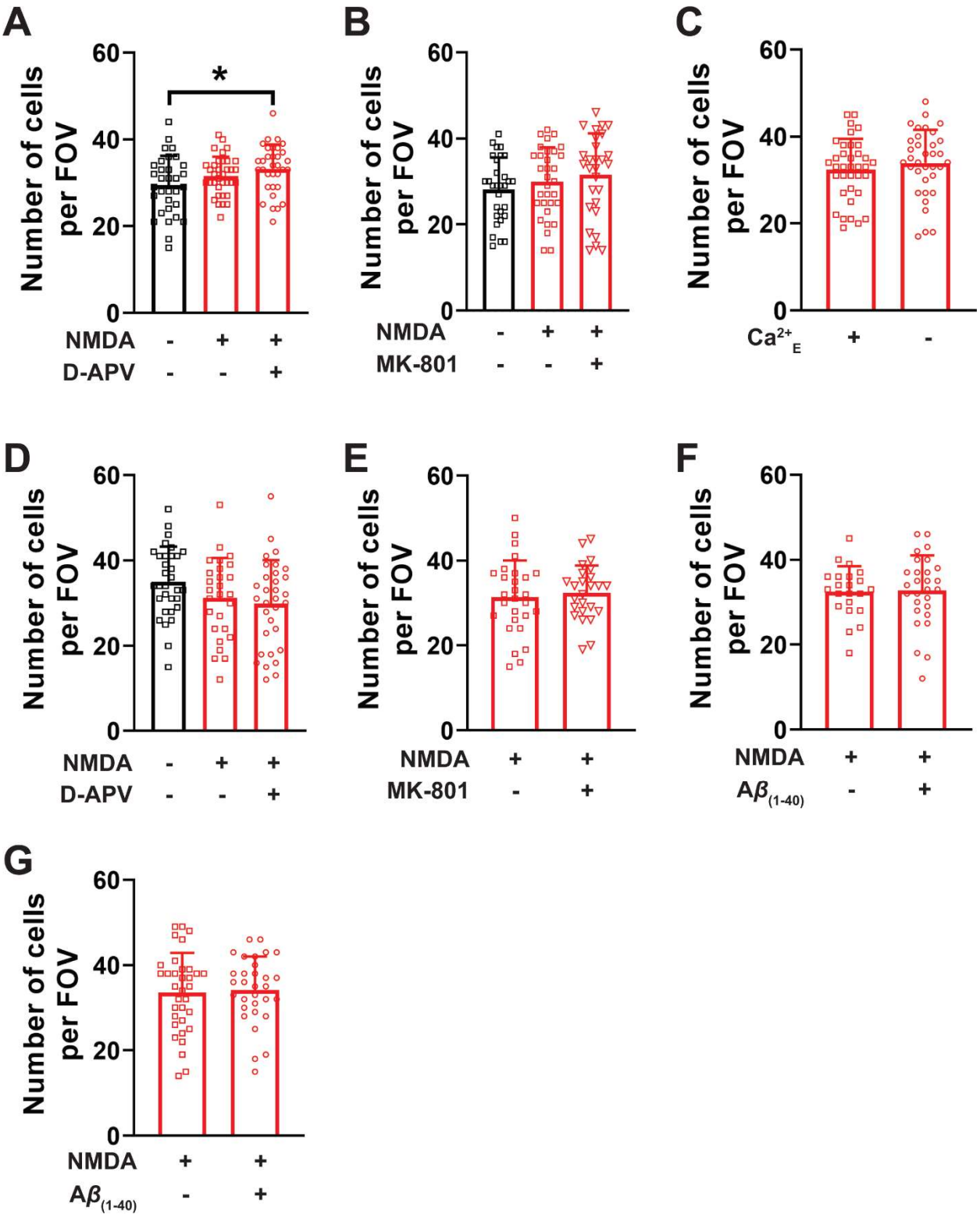

Supplemental Figure 7. *Number of cells per field of view (FOV) for each Ca^{2+} imaging experiment*. Bar graph depicting the mean ± SD of the number of endothelial cells per FOV in experiments shown in Figure 1 **(A)**, Supplemental Figure 1 **(B)**, Supplemental Figure 2 **(C)**, Figure 2 **(D)**, Supplemental Figure 5 **(E)**, Figure 4 **(F)**, and Figure 5 **(G)**. For the experiments corresponding to Figure 1, there was a significant difference in number of cells per field of view between vehicle and NMDA + D-APV treatment groups (*$p < 0.05$, ordinary one-way ANOVA). No significant differences were observed in the number of cells per FOV between treatment groups for any other experiments. A$\beta_{(1\text{-}40)}$: amyloid-$\beta_{(1\text{-}40)}$.

Supplemental Figure 8. Myogenic tone in various treatments.

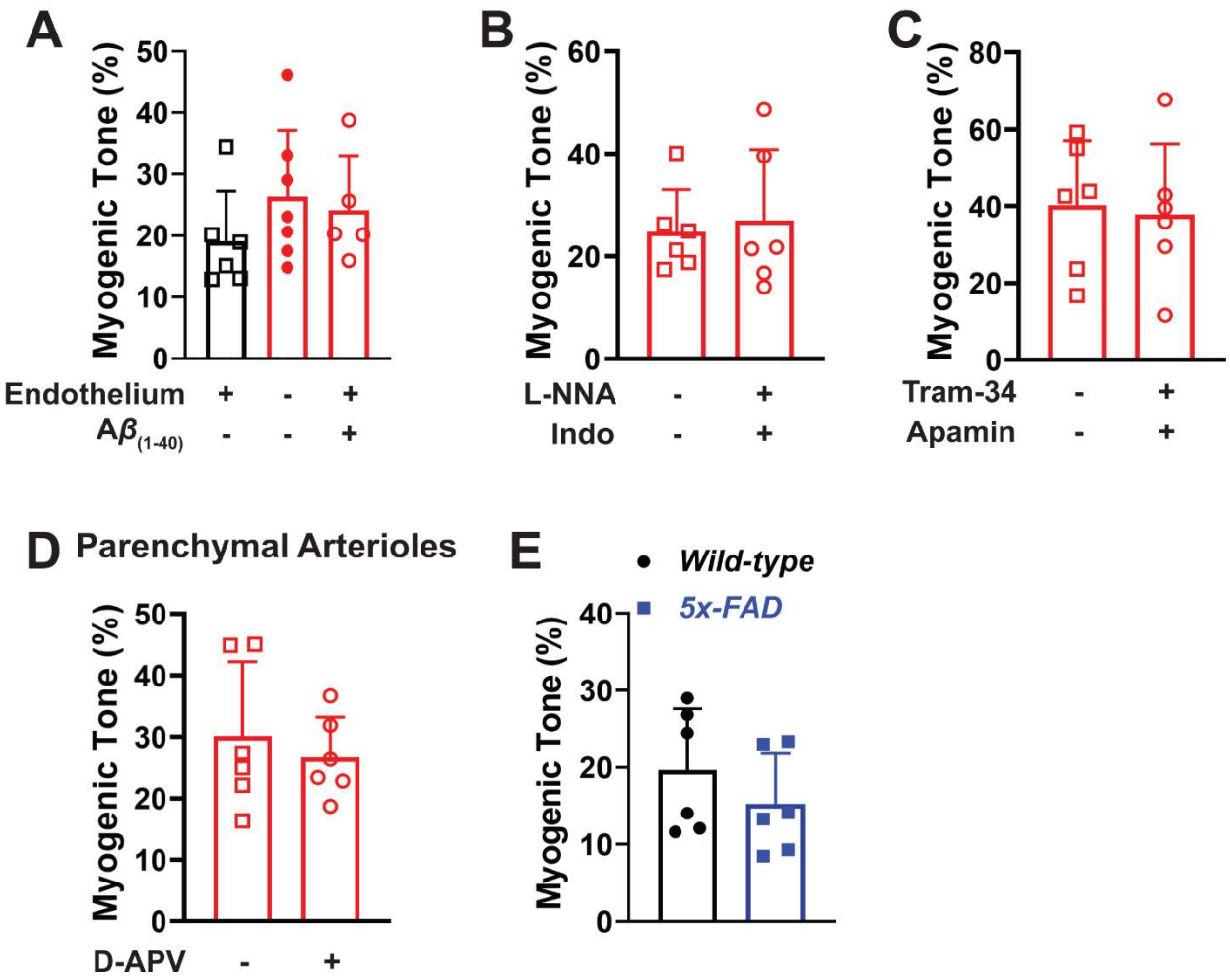

Supplemental Figure 8. *Myogenic tone in various treatments.* **(A-C)** Summary bar graphs depicting that there were no significant differences in myogenic tone between treatment groups for wild-type pial arteries. **(D)** Summary bar graph showing that DAPV did not affect myogenic tone in parenchymal arterioles isolated from wild-type mice. **(E)** Summary bar graph showing that there was no significant difference in myogenic tone between wild-type and *5x-FAD* pial arteries. Data are means ± SD.

Supplemental Figure 9. Summary diagram

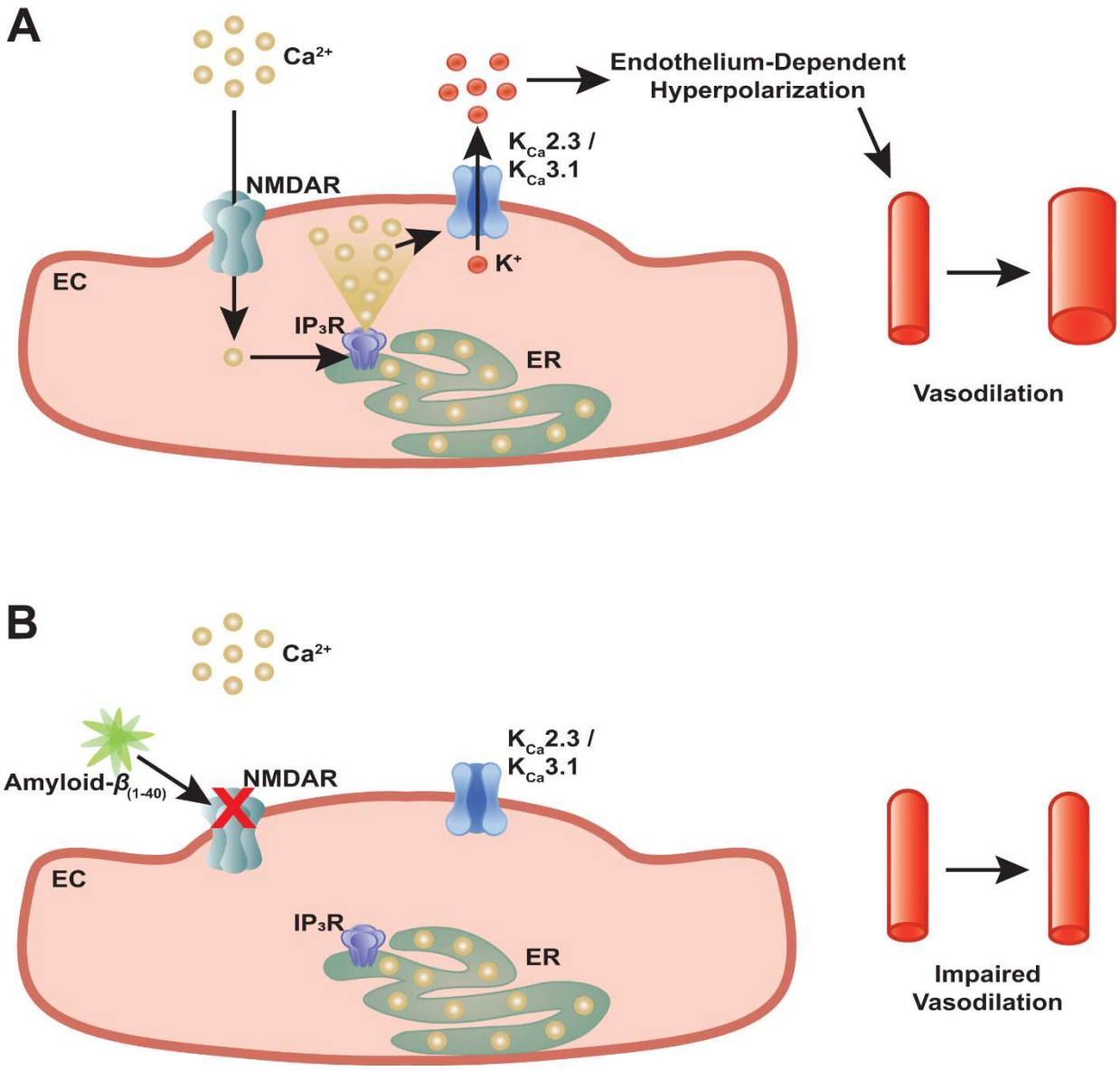

Supplemental Figure 9. *Summary figure.* **(A)** Proposed mechanism for how activation of the endothelial NMDAR induces vasodilation via endothelium-dependent hyperpolarization. **(B)** Proposed schematic for how amyloid-$\beta_{(1\text{-}40)}$ impairs activity of the endothelial NMDAR, resulting in impaired vasodilation.

Legends for Supplemental Movies.

Movie S1. *Spontaneous Ca^{2+} influx in cerebral artery endothelial cells from cdh5:Gcamp8 mice.* Representative movie of a 512 x 512 pixels field of view of an *en face* cerebral artery from *cdh5:Gcamp8* mouse pre-incubated with EGTA-AM (10 μmol/L) and cyclopiazonic acid (CPA, 10 μmol/L) and exposed to vehicle. Bar = 20 μm.

Movie S2. *NMDAR sparklets in cerebral artery endothelial cells.* Representative movie of the same field of view from Movie S1 showing that addition of NMDA (10 μmol/L) to the superfusate elicits Ca^{2+} influx events in cerebral artery endothelial cells. Preparation was pre-incubated with EGTA-AM (10 μmol/L) and cyclopiazonic acid (CPA, 10 μmol/L) to prevent Ca^{2+} release from intracellular stores. Bar = 20 μm.

Movie S3. *NMDAR sparklets are inhibited by the NMDAR antagonist D-APV in cerebral artery endothelial cells.* Representative movie of the same field of view from Movies S1 and S2 showing the NMDAR antagonist D-APV (10 μmol/L) reduces the number of *NMDAR sparklets* in cerebral artery endothelial cells. Preparation was pre-incubated with EGTA-AM (10 μmol/L) and cyclopiazonic acid (CPA, 10 μmol/L) to prevent Ca^{2+} release from intracellular stores. Bar = 20 μm.

Movie S4. *Intracellular Ca^{2+} transients in cerebral artery endothelial cells from cdh5:Gcamp8 mice.* Representative movie of a 512 x 512 pixels field of view from an *en face* cerebral artery showing spontaneous Ca^{2+} transients when exposed to vehicle (imaging PSS). Bar = 20 μm.

Movie S5. *NMDA increases the frequency of intracellular Ca^{2+} transients in cerebral artery endothelial cells.* Representative movie from the same field of view as Movie S4 showing that addition of NMDA (10 μmol/L) to the superfusing imaging PSS increases the frequency of intracellular Ca^{2+} transients in cerebral artery endothelial cells. Bar = 20 μm.

Movie S6. *D-APV inhibits NMDA-induced increases in intracellular Ca^{2+} transients in cerebral artery endothelial cells.* Representative movie from the same field of view as Movies S4 and S5 showing that addition of D-APV (10 μmol/L) to the superfusing imaging PSS prevents the observed increase in the frequency of intracellular Ca^{2+} transients induced by NMDA. Bar = 20 μm.

Movie S7. *NMDAR sparklets in cerebral artery endothelial cells.* Representative movie of a field of view from a different preparation showing *NMDAR sparklets* elicited by NMDA (10 μmol/L) in cerebral artery endothelial cells. Preparation was pre-incubated with EGTA-AM (10 μmol/L) and cyclopiazonic acid (CPA, 10 μmol/L) to prevent Ca^{2+} release from intracellular stores. Bar = 20 μm.

Movie S8. *Amyloid-$\beta_{(1\text{-}40)}$ inhibits NMDAR sparklets in cerebral artery endothelial cells.* Representative movie of the same field of view as Movie S7 showing that incubating the preparation with amyloid-$\beta_{(1\text{-}40)}$ (5 μmol/L) inhibits NMDA from eliciting *NMDAR sparklets* in cerebral artery endothelial cells. Preparation was also pre-incubated with EGTA-AM

(10 μmol/L) and cyclopiazonic acid (CPA, 10 μmol/L) to prevent Ca^{2+} release from intracellular stores. Bar = 20 μm.

Movie S9. *NMDAR-induced intracellular Ca^{2+} transients in endothelial cells from cerebral arteries.* Representative movie of a 512 x 512 field of view from a different *en face* preparation showing intracellular Ca^{2+} transients after exposure to NMDA (10 μmol/L) in the superfusing imaging PSS. Bar = 20 μm.

Movie S10. *Amyloid-$\beta_{(1-40)}$ prevents NMDA from increasing the frequency of intracellular Ca^{2+} transients in cerebral artery endothelial cells.* Representative movie of the same field of view as Movie S9 showing that incubating the preparation with amyloid-$\beta_{(1-40)}$ (5 μmol/L) prevents NMDA from increasing the number of intracellular Ca^{2+} transients in cerebral artery endothelial cells from *cdh5:Gcamp8* mice. Bar = 20 μm.